

A simplified type-2 fuzzy logic controller for real-time control

Dongrui Wu Woei Wan Tan*

^a*Department of Electrical and Computer Engineering, National University of Singapore, 4, Engineering Drive 3, Singapore 117576, Singapore*

(Received 23 February 2005; accepted 3 November 2005)

Abstract

Increasingly, genetic algorithms (GAs) are used to optimize the parameters of fuzzy logic controllers (FLCs). Although GAs provide a systematic design approach, the optimization process is generally performed off-line using a plant model. Differences between the model and physical plant may result in unsatisfactory control performance when the FLCs are deployed in practice. Type-2 FLCs are an attractive alternative because they can better cope with modeling uncertainties. Unfortunately, type-2 FLCs are computationally intensive. This paper presents a simplified type-2 FLC that is suitable for real-time applications. The key idea is to only replace some critical type-1 fuzzy sets by type-2 sets. Experimental results indicate that the proposed simplified type-2 FLC is as robust as a conventional type-2 FLC, while lowering the computational cost. © 2006 ISA—The Instrumentation, Systems, and Automation Society.

Keywords: Type-2 fuzzy logic; Robust control

1. Introduction

Fuzzy logic controllers (FLCs) are usually constructed using type-1 fuzzy sets [1], referred to as type-1 FLCs. Such FLCs have been applied to many areas [2], especially for the control of complex nonlinear systems that are difficult to model analytically [3,4]. Despite their popularity, research has shown that type-1 FLCs may have difficulties in modeling and minimizing the effect of uncertainties [5,6]. This limitation may restrict the usefulness of design methods that tune the FLCs using the genetic algorithm (GA) and a model of the controlled process. Since it is impossible for a model to capture all the characteristics of the actual plant, the performance of a controller designed using a model will inevitably deteriorate when it is applied to the practical system. A con-

troller that is equipped with the ability to handle more modeling uncertainties would be valuable.

Type-2 fuzzy sets, characterized by membership grades that are themselves fuzzy, were introduced by Zadeh in 1975 [7] to better handle uncertainties. As illustrated in Fig. 1, the membership function (MF) of a type-2 set has a footprint of uncertainty (FOU), which represents the uncertainties in the shape and position of the type-1 fuzzy set. The FOU is bounded by an upper MF and a lower MF, both of which are type-1 MFs.

Fuzzy logic systems (FLSs) constructed using rule bases that utilize at least one type-2 fuzzy sets are called type-2 FLSs. Since the FOU of a type-2 fuzzy set provides an extra mathematical dimension, type-2 FLSs can better handle system uncertainties and have the potential to outperform their type-1 counterparts. Type-2 FLSs have been used successfully in many applications, for example, time-series forecasting [8,5], communication and networks [9,10], decision making [11,12], data

*Tel.: +65 6516 8323; fax: +65 6779 1103. E-mail address: wwtan@nus.edu.sg

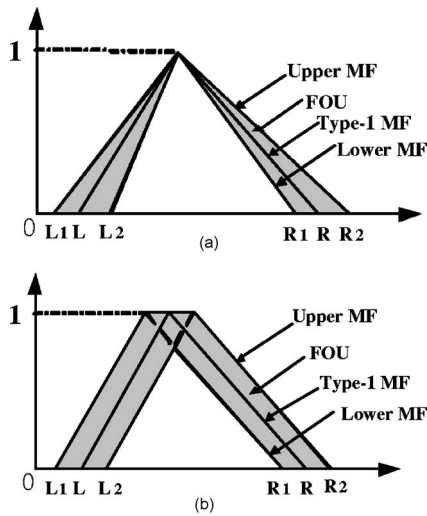


Fig. 1. Examples of type-2 fuzzy sets. (a) A type-2 fuzzy set obtained by blurring the width of a triangular type-1 fuzzy set and (b) a type-2 fuzzy set obtained by blurring the apex of a triangular type-1 fuzzy set.

and survey processing [13,5], word modeling [14,15], phoneme recognition [16], plant monitoring and diagnostics [17], etc. Even though fuzzy control is the most widely used application of fuzzy set theory, a literature search reveals that only a few type-2 FLSs are employed in the field of control. Interval type-2 FLCs were applied to mobile robot control [6], quality control of sound speakers [18], connection admission control in ATM networks [19]. A dynamical optimal training algorithm for type-2 fuzzy neural networks (T2FNNs) has also been proposed [20]. T2FNNs have been used in nonlinear plant control [21] and truck back up control [20].

The structure of a typical type-2 FLC is shown in Fig. 2. Input signals are the feedback error e and the change of error \dot{e} , and the output is the change of control signal \dot{u} . Compared with their type-1 counterparts, type-2 FLCs are better suited to eliminate persistent oscillations [22–24]. The most likely explanation for this behavior is a

type-2 FLC has a smoother control surface than that of a type-1 FLC, especially around the origin. Hence, small disturbances around steady state will not result in significant control signal changes so there are less oscillations. As the ability of type-2 FLCs to handle modeling uncertainties is superior, a type-2 FLC evolved using the GA and the plant model is more likely to perform well in practice. Despite the advantages offered by type-2 FLCs, one problem that may hinder the use of type-2 FLCs for real-time control is their high computational cost. Unlike a type-1 FLC, a type-reducer is needed to convert the type-2 fuzzy output sets into type-1 sets so that they can be processed by the defuzzifier to give a crisp output. Type-reduction is very computationally intensive, especially when there are many MFs and the rule base is large. To reduce the computational burden while preserving the advantages of type-2 FLCs, two approaches may be considered: (1) faster type-reduction methods, such as the uncertainty bound concept in Ref. [25] and new type-reducers proposed in Ref. [26]; and (2) a simpler architecture. The second approach is studied herein. A procedure to obtain a type-2 FLC that is robust enough to cope well with the uncertainties while having minimum computational cost is proposed. This paper also presents experimental study that establishes the feasibility of the proposed simplified type-2 structure.

The rest of the paper is organized as follows: Section 2 introduces a traditional type-2 FLC and discusses the merits as well as the limitations of the controller. The proposed simplified type-2 FLC as well as a computational costs comparison are presented in Section 3. Two type-1 FLCs and two type-2 FLCs with different degrees of freedom are designed in Section 4 and their abilities to handle modeling uncertainties are compared using a coupled-tank liquid-level control system. Sec-

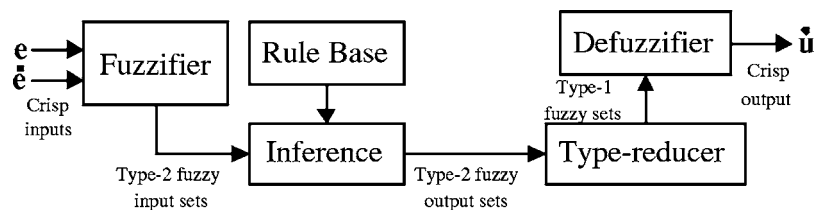


Fig. 2. Scheme of a type-2 FLC.

tion 5 discusses the performances of the proposed architecture. Finally, conclusions are drawn in Section 6.

2. Type-2 FLC

Most research conducted thus far has concentrated on interval singleton type-2 FLSs [5]. The term “interval” indicates that only interval type-2 fuzzy sets, where all points in the FOU have unity secondary membership grades, are utilized. “Singleton” denotes that the fuzzifier converts the input signals of the FLC into fuzzy singletons. This class of type-2 FLSs is popular because the remaining types can be computationally very costly. In this paper, interval singleton type-2 FLSs with the input-output structure of a Mamdani fuzzy proportional plus integral (PI) controller are studied.

Consider a two-inputs single-output type-2 FLS. The inputs are the feedback error, e , and the change of the error, \dot{e} , while the output signal is the change in the control signal, \dot{u} . The e domain is partitioned by N ($N=2m-1, m>0$) type-2 fuzzy sets that are labeled as $\tilde{F}_1^i (i=1, 2, \dots, N)$. \dot{e} domain is also partitioned by N type-2 sets, labeled as $\tilde{F}_2^j (j=1, 2, \dots, N)$. Assuming that there is a rule for each possible combination of the N sets in the two input domains, then the rule base comprises of N^2 rules. The k th $\{k=N(i-1)+j, k \in [1, N^2]\}$ rule assumes the following form:

R^k : if e is \tilde{F}_1^i and \dot{e} is \tilde{F}_2^j , then \dot{u} is $Z^k (i, j = 1, 2, \dots, N)$.

Each consequent set, Z^k , is a distinct type-1 fuzzy set. Just as the sup-star composition is the backbone of the inference engine of a type-1 FLC, the extended supstar composition is the backbone of a type-2 FLC. When the meet operation is implemented by the product t -norm, the firing set associated with the k th rule is the following interval type-1 set

$$F^k(e, \dot{e}) = [\underline{f}^k(e, \dot{e}), \bar{f}^k(e, \dot{e})], \quad (1)$$

where $\underline{f}^k(e, \dot{e}) = \underline{\mu}_{\tilde{F}_1^i}(e) \times \underline{\mu}_{\tilde{F}_2^j}(\dot{e})$ and $\bar{f}^k(e, \dot{e}) = \bar{\mu}_{\tilde{F}_1^i}(e) \times \bar{\mu}_{\tilde{F}_2^j}(\dot{e})$. $\underline{\mu}_{\tilde{F}_1^i}(e)$ and $\bar{\mu}_{\tilde{F}_1^i}(e)$ are the lower and upper membership grades of the interval firing set $\mu_{\tilde{F}_1^i}(e)$. $\underline{\mu}_{\tilde{F}_2^j}(\dot{e})$ and $\bar{\mu}_{\tilde{F}_2^j}(\dot{e})$ are the lower and upper membership grades of the interval firing set

$\mu_{\tilde{F}_2^j}(\dot{e})$. Next, the firing set, $F^k(e, \dot{e})$, is combined with the consequent fuzzy set of the k th rule using the product t -norm to derive the fired output consequent sets.

By using the maximum t -conorm, the combined output fuzzy set may then be obtained. Unlike type-1 FLSs, the output of the inference engine must be type reduced before the defuzzifier can be used to generate a crisp output. The most commonly used type-reduction method is the center-of-sets type-reducer, which is based on the generalized centroid concept [5]. For the interval singleton type-2 FLC, the type-reduced set is

$$\dot{U}_{\text{cos}} = \int_{z_1 \in Z^1} \cdots \int_{z_{N^2} \in Z^{N^2}} \int_{f_1 \in F^1} \cdots \int_{f_{N^2} \in F^{N^2}} \left| \begin{array}{c} N^2 \\ \sum_{k=1} z_k f_k \\ \frac{k=1}{N^2} \\ \sum_{k=1} f_k \end{array} \right| = [\dot{u}_l, \dot{u}_r], \quad (2)$$

where $F^k(e, \dot{e})$ is the interval type-1 set with center h_k and spread δ_k as defined in Eq. (1). Z_k is a type-1 fuzzy set with center c_k and spread s_k . The center-of-sets type-reducer is widely used because Eq. (2) may be computed using the Karnik-Mendel iterative method [5]

Set $z_k = c_k - s_k$ ($z_k = c_k + s_k$) for $k=1, \dots, N^2$;
 Arrange z_k in ascending order;
 Set $w_k = h_k$ for $k=1, \dots, N^2$;

$$\dot{u}' = \frac{\sum_{k=1}^{N^2} z_k w_k}{\sum_{k=1}^{N^2} w_k};$$

do

$\dot{u}'' = \dot{u}'$;
 Find $p \in [1, N^2 - 1]$ such that $z_p \leq \dot{u}' \leq z_{p+1}$;
 Set $w_k = h_k + \delta_k$ ($w_k = h_k - \delta_k$) for $k \leq p$;
 Set $w_k = h_k - \delta_k$ ($w_k = h_k + \delta_k$) for $k \geq p+1$;

$$\dot{u}' = \frac{\sum_{k=1}^{N^2} z_k w_k}{\sum_{k=1}^{N^2} w_k};$$

while $\dot{u}' \neq \dot{u}''$

$\dot{u}_l(\dot{u}_r) = \dot{u}'$.

It has been proven that the Karnik-Mendel iterative procedure can be completed in at most N^2 iterations [5]. Once \dot{u}_l and \dot{u}_r are obtained, the type-reduced set can be defuzzified to calculate the crisp output. For an interval type-reduced set, the defuzzified output is

$$\dot{u} = \frac{\dot{u}_l + \dot{u}_r}{2}.$$

Interval singleton type-2 PI-like FLC has been tested on non-linear systems [22,23]. The main strength of such type-2 FLCs is their ability to eliminate persistent oscillations, and thus enabling them to tolerate more modeling uncertainties. It is also found that the control surface of type-2 FLCs around the steady state is smoother than that of type-1 FLCs. This means that small disturbances around steady state will not result in significant control signal changes so the amount of oscillations is reduced. Unfortunately, the ability to better handle modeling uncertainties is accompanied by significantly larger computing requirement. To address this limitation, a type-2 FLC that can be implemented with lower computational cost is proposed in the following section.

3. Simplified type-2 FLCs

The simplified interval singleton type-2 FLC is one that uses type-2 fuzzy set(s) only for the fuzzy partition(s) governing behavior around the set-point (steady state). All other fuzzy sets are type-1. Figs. 3(c) and 3(d) show the MFs of a typical simplified type-2 FLCs. The structure is motivated by the observation that the main advantage of type-2 FLC is its ability to provide more damping as the output approaches the set point. It is conjectured that the degradation in the ability of a type-2 FLC to handle modeling uncertainties will be insignificant if type-1 fuzzy sets are used to describe the fuzzy rules that govern the transient response. Such a simplified structure and a FLC where all the fuzzy sets used to partition the input domains are type-2 may have similar control surfaces around the origin. As the control surfaces are comparable, it is likely that these two kinds of FLCs may have similar performances. The computational cost of the proposed controller will be lower since the simplified architecture utilizes fewer type-2 sets.

A simplified type-2 FLC may be designed by gradually replacing type-1 fuzzy sets by their type-2 counterpart until the resulting FLC meets

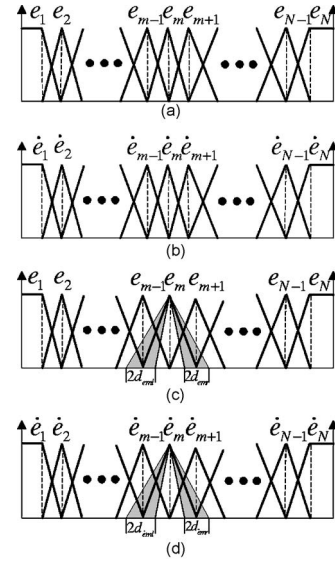


Fig. 3. Example MFs of the FLCs. (a) MFs of e , which are all type-1; (b) MFs of \dot{e} , which are all type-1; (c) MFs of e . Here the middle one (the m th MF) is type-2 while all the others are type-1; and (d) MFs of \dot{e} . Here the middle one (the m th MF) is type-2 while all the others are type-1.

the robustness requirements, starting with the fuzzy sets that characterize the region around steady state. Since the computational cost will increase significantly when the number of type-2 MFs increases, as few type-2 MFs as possible should be introduced. For a PI-like FLC, the response near steady state is determined mainly by the area around the origin, which is governed by the middle MFs of each input. Hence, the procedure for designing a simplified type-2 FLC is as follows:

Step 1: The type-1 FLC is designed through simulation on a nominal model.

Step 2: Change the most important input MF to type-2. For the two inputs of a PI-like FLC, \dot{e} is more susceptible to noises. The fuzzy set corresponding to zero \dot{e} is changed to type-2, as illustrated in Fig. 3(d).

Step 3: If the type-2 FLC designed in step 2 cannot cope well with the actual plant, the fuzzy set associated with zero e is changed to type-2, as illustrated in Fig. 3(c).

Step 4: If the resulting type-2 FLC is still not robust enough, more type-2 MFs may be introduced starting from the middle of each input domain and gradually moving towards the limits of the domain. Another criteria is to use type-2 fuzzy

sets to characterize the operating region that needs a smoother control surface.

A FLC designed by the proposed procedure has two parts—a type-1 part and a type-2 part. Different fuzzy partitions will be activated when the state of the plant is in different operating region. During the transient stage, the FLC behaves like a type-1 FLC since no type-2 MFs are fired. When the output approaches the setpoint, type-2 MFs will be fired and the plant is controlled by a type-2 FLC. Smoother control signals will be generated, which help to eliminate oscillations. Next, an analysis is performed in order to establish the computational savings provided by the simplified type-2 FLC.

3.1. Computational cost comparison

The reduction in computational requirement comes about mainly because the simplified structure enables type-reduction algorithm to be simplified. Consider a simplified type-2 FLC where M out of the N^2 rules contain only type-1 MF in the antecedent. The remaining $N^2 - M$ rules have at least one type-2 fuzzy set in the antecedent. There will, therefore, be M crisp firing strengths (f_i , $i = 1, 2, \dots, M$) and $N^2 - M$ interval firing strengths (\tilde{f}_j , $j = M + 1, M + 2, \dots, N^2$). In this case, Eq. (2) reduces to

$$\begin{aligned} \dot{U}_{\cos} &= \frac{\sum_{i=1}^M z_i f_i + \sum_{j=M+1}^{N^2} z_j \tilde{f}_j}{\sum_{i=1}^M f_i + \sum_{j=M+1}^{N^2} \tilde{f}_j} = \frac{\beta + \sum_{j=M+1}^{N^2} z_j \tilde{f}_j}{\alpha + \sum_{j=M+1}^{N^2} \tilde{f}_j} \\ &= \frac{\beta}{\alpha} + \frac{\sum_{j=M+1}^{N^2} z_j \tilde{f}_j - \frac{\beta}{\alpha} \sum_{j=M+1}^{N^2} \tilde{f}_j}{\alpha + \sum_{j=M+1}^{N^2} \tilde{f}_j} \\ &= \frac{\beta}{\alpha} + \frac{\sum_{j=M+1}^{N^2} \left(z_j - \frac{\beta}{\alpha} \right) \tilde{f}_j}{\alpha + \sum_{j=M+1}^{N^2} \tilde{f}_j}, \end{aligned} \quad (3)$$

where $\alpha = \sum_{i=1}^M f_i$, $\beta = \sum_{i=1}^M z_i f_i$.

Defining z'_j and \tilde{f}_{N^2+1} as

$$z'_j = \begin{cases} z_j - \frac{\beta}{\alpha}, & j = M + 1, M + 2, \dots, N^2 \\ 0, & j = N^2 + 1 \end{cases}$$

$$\tilde{f}_{N^2+1} = \alpha.$$

Eq. (3) can be further simplified to

$$\dot{U}_{\cos} = \frac{\beta}{\alpha} + \frac{\sum_{j=M+1}^{N^2+1} z'_j \tilde{f}_j}{\sum_{j=M+1}^{N^2+1} \tilde{f}_j}. \quad (4)$$

The second term on the right hand side of Eq. (4), $\sum_{j=M+1}^{N^2+1} z'_j \tilde{f}_j / \sum_{j=M+1}^{N^2+1} \tilde{f}_j$, can be calculated by the Karnik-Mendel iterative method. Once α and β are calculated, the Karnik-Mendel type-reducer will converge in at most $(N^2 + 1 - M)$ iterations because the number of interval firing strengths has been reduced from N^2 to $(N^2 + 1 - M)$.

To further investigate the savings in computational cost provided by the simplified type-2 FLCs, the computing requirements of one type-1 FLC (FLC₁) and three different type-2 FLCs (FLC_{2s}, FLC_{2m}, and FLC_{2f}) are compared qualitatively. The FLCs have two input signals (e and \dot{e}). Each input domain is characterized by N fuzzy sets that are equally spaced and the output domain has N^2 fuzzy sets. FLC_{2s} is a type-2 FLC where only the middle MF of \dot{e} is type-2 (corresponds to step 2 of the design procedure). Its input MFs are shown in Figs. 3(a) and 3(d). FLC_{2m} is one where the middle MF of both e and \dot{e} are type-2. This FLC is the result of step 3 of the design procedure and its input MFs are shown in Figs. 3(c) and 3(d). All the input MFs of FLC_{2f} are type-2. The performances of the three type-2 FLCs are compared with a type-1 FLC, whose input MFs are shown in Figs. 3(a) and 3(b).

The comparative study was performed by first dividing the domain of e , $[-1, 1]$, into 101 equally distributed points e_i , where $e_i = 2(i-1)/100 - 1$ ($i = 1, 2, \dots, 101$). 101 \dot{e}_i are generated in the same way. Thus, all possible combinations of e_i and \dot{e}_i yield 10 201 input pairs. Computational cost is evaluated by comparing the time needed to find outputs for these 10 201 inputs. All the experiments are done by Matlab on a 996 MHz computer with 256 MB of random access memory (RAM) and Windows XP. The Karnik-Mendel iterative type-reduction method used is the standard routine downloaded from the web [27]. Table 1 shows the results for different values of N . The data indicate that the computations for the proposed structure is completed in less than half the time required for a full type-2 FLC. Computa-

Table 1
Computational cost of the 4 FLCs.

$N \backslash \text{FLC}$	FLC_1 (s)	FLC_{2s} (s)	FLC_{2m} (s)	FLC_{2f} (s)
3	1.2	2.0	6.7	10.4
5	1.6	2.5	5.1	10.3
7	2.3	3.7	5.0	12.0
9	3.3	5.6	6.6	15.0
11	4.6	8.6	9.5	19.6

tional saving is also much larger when N is small. Having shown that the computing requirements of the simplified type-2 FLC is less, the control performance of the proposed structure is examined in the following section.

4. Liquid level control experiments

In this section, the GA-based strategy that was employed to tune the parameters of FLCs is described. Four FLCs (FLC_{13} , FLC_{15} , FLC_{2s} , and FLC_{2f}) are evolved and tested on a coupled-tank system, a nonlinear SISO time-delay system. Fig. 4 shows the schematic diagram of the coupled-tank while a description of the simulation model is in the Appendix.

4.1. Structure of the FLCs

Of the four FLCs that were designed, three FLCs (FLC_{13} , FLC_{2s} , and FLC_{2f}) have essentially the same architecture. The only difference is that the input domains of FLC_{13} (e and \dot{e}) are partitioned by type-1 sets, while that of the type-2 FLCs are partitioned by at least one type-2 set. Each input domain is partitioned by three fuzzy MFs that are labeled as **N**, **Z**, and **P**. The output space (\dot{u}) has five MFs labeled as **NB**, **NS**, **Z**, **PS**, and **PB**. As illustrated in Fig. 1, a type-2 fuzzy set can be obtained by blurring the MF of a base line type-1 set. For a triangular type-1 MF, there are at

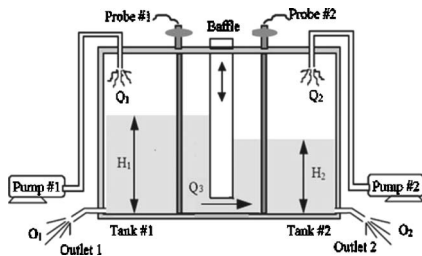


Fig. 4. The coupled-tank liquid-level control system.

Table 2
Rule base of FLC_{13} , FLC_{2s} , and FLC_{2f} .

$e \backslash \dot{e}$	$N_{\dot{e}}$	$Z_{\dot{e}}$	$P_{\dot{e}}$
N_e	NB	NS	Z
Z_e	NS	Z	PS
P_e	Z	PS	PB

least two ways of blurring to obtain a type-2 MF. The first is to keep the apex fixed while blurring the width of the triangle, as shown in Fig. 1(a). The other way is to keep the width of the triangle fixed while blurring the apex, as shown in Fig. 1(b). The first approach is employed in this paper. Table 2 shows the fuzzy rule base used by the four FLCs. It is commonly used to construct FLCs. The various fuzzy set operations adopted in this paper are the sum-product inference engine, center-of-sets type-reducer and height defuzzifier.

Since each type-2 set provides an extra mathematical dimension, the type-2 FLCs have more degrees of freedom than FLC_{13} . It is generally known that a FLC with more parameters tends to provide better performance. In order to investigate whether the simplified type-2 FLC is able to outperform a type-1 FLC with a similar number of design parameters, another type-1 FLC (FLC_{15}) is included in the comparative study. It has five MFs in each input domain and the rule base is shown in Table 3.

4.2. GA coding scheme and parameters

The parameters of the four FLCs used in this study are evolved by GA, a general-purpose search algorithm that is based on the mechanics of natural selection and genetics. It was first proposed in 1975 [28]. GAs are theoretically and empirically proven to be a robust search engine in complex spaces, thereby offering a valid approach to problems requiring efficient and effective

Table 3
Rule base of FLC_{15} .

$e \backslash \dot{e}$	\dot{e}_1	\dot{e}_2	\dot{e}_3	\dot{e}_4	\dot{e}_5
e_1	\dot{u}_1	\dot{u}_2	\dot{u}_3	\dot{u}_4	\dot{u}_5
e_2	\dot{u}_2	\dot{u}_3	\dot{u}_4	\dot{u}_5	\dot{u}_6
e_3	\dot{u}_3	\dot{u}_4	\dot{u}_5	\dot{u}_6	\dot{u}_7
e_4	\dot{u}_4	\dot{u}_5	\dot{u}_6	\dot{u}_7	\dot{u}_8
e_5	\dot{u}_5	\dot{u}_6	\dot{u}_7	\dot{u}_8	\dot{u}_9

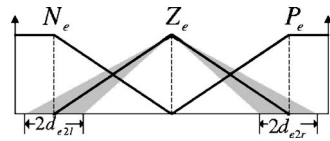


Fig. 5. Example MFs of e .

searches [29–32]. The key idea behind the search process is inspired by the natural evolution of biological creatures, where the fittest among a group of artificial entities survive to form a new generation together with those that are produced through gene exchange. Given an initial population of candidate solutions that are represented as strings called chromosomes, GAs operate in cycles known as generations. For each generation, the fitness of all individuals with respect to the optimization task is evaluated via a scalar objective function (fitness function), and the result of this evaluation is used to drive the Darwinian selection process. A certain percentage of every generation is also produced randomly via genetic operators such as crossover and mutation to provide genetic diversity, and thus increasing the probability of finding the global minimal.

Although the GA is increasingly used to facilitate FLSS design, most existing works only touch on the design of type-1 systems [33–36]. In this paper, GAs are used to tune both type-1 and type-2 FLCs. First, the chromosome coding scheme is described. Since the input domain of FLC₁₃ is partitioned by three MFs, three points are needed to determine the MFs of each input. The three points for the e domain are N_e , Z_e , and P_e , as illustrated in Fig. 5. Similarly, the three points that define the three sets for the \dot{e} domain are $N_{\dot{e}}$, $Z_{\dot{e}}$, and $P_{\dot{e}}$. Another five points are needed to determine the MFs of the output domain, \dot{u} . Consequently, there is a total of 11 parameters which need to be optimized by the GA.

Fig. 6 shows the chromosome used by the GA, where the first 11 genes are parameters of FLC₁₃. The next two genes in the chromosome determine the FOU of the only type-2 set used to partition the \dot{e} domain of FLC_{2c}. They define the amount by

Table 4

Plants used to assess fitness of candidate solutions.

	Plant I	Plant II	Plant III	Plant IV
$A_1=A_2$ (cm ²)		36.52		
$\alpha_1=\alpha_2$		5.6186		
α_3	10	10	10	8
Setpoint (cm)	0 → 15	0 → 22.5 → 7.5	0 → 15	0 → 15
Transport delay (s)	0	0	2	0

which the type-1 set is shifted ($d_{\dot{e}2l}$ and $d_{\dot{e}2r}$) to generate the FOU of the type-2 fuzzy set. In the case of FLC_{2f}, the input domains are partitioned by six type-2 sets so the chromosome has 19 genes, as shown in Fig. 6. Finally for FLC₁₅, five parameters are needed to determine the MFs for each input and nine parameters for the consequents. Thus, each chromosome consists of $5 \times 2 + 9 = 19$ genes, the same as that of FLC_{2f}.

The fitness of each chromosome in the GA population is assessed by subjecting the simulation model of the liquid level process (refer to the appendix) to step inputs. As this paper aims at exploring the abilities of the four FLCs to handle modeling uncertainties, each candidate solution is used to control plants with the four sets of parameters shown in Table 4. The integral of time absolute error (ITAE) obtained for each of the four plants are added together [see Eq. (5)] and used to evaluate the fitness of the FLCs

$$F = \sum_{i=1}^4 \alpha_i \left[\sum_{j=1}^{N_i} j * |e_i(j)| \right], \quad (5)$$

where α_i is the weight corresponding to the ITAE of the i th plant, and $N_i=200$ is the number of sampling instants. There is a need to introduce α_i because the ITAE of the second plant is usually several times bigger than that of other plants. To ensure that the ITAE of the four plants can be reduced with equal emphasis, α_2 is defined as 1/3 while the other weights are unity.

1	2	3	4	5	6	7	8	9	10	11	12	13	14	15	16	17	18	19
N_e	Z_e	P_e	$N_{\dot{e}}$	$Z_{\dot{e}}$	$P_{\dot{e}}$	NB	NS	Z	PS	PB	$d_{\dot{e}2l}$	$d_{\dot{e}2r}$	d_{e2l}	d_{e2r}	$d_{\dot{e}1r}$	$d_{\dot{e}3l}$	d_{e1r}	d_{e3l}
Sub-chromosome of e			Sub-chromosome of \dot{e}			Sub-chromosome of \dot{u}												

Fig. 6. GA coding scheme of the FLCs.

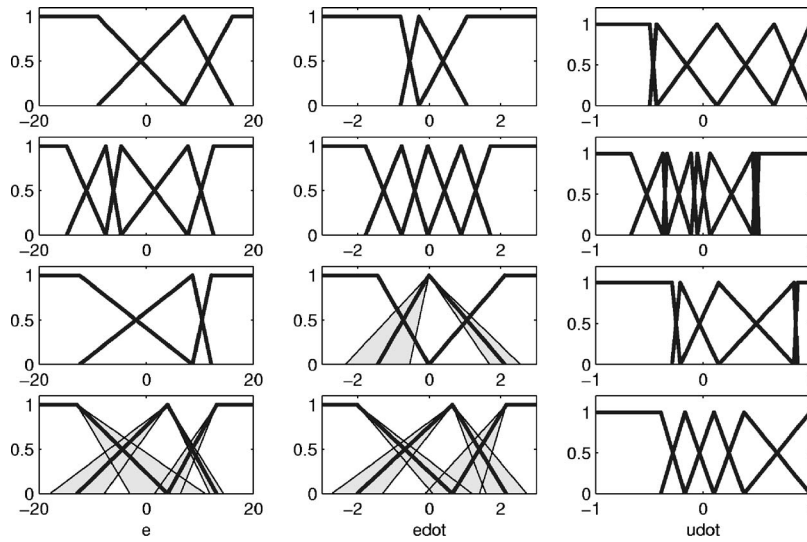


Fig. 7. MFs of the four FLCs (FLC₁₃, FLC₁₅, FLC_{2s}, and FLC_{2f}, from the top to the bottom).

The GA consisted of 200 chromosomes in each generation and terminated after 100 generations. The crossover rate was 0.8 and the mutation rate was 0.1. The MFs of FLC₁₃, FLC₁₅, FLC_{2s}, and FLC_{2f} evolved by GA are shown in Fig. 7. The parameters are listed in Table 5 and Table 6.

4.3. Experimental results

This section presents results from the simulation and experimental study that was conducted to assess the performance of the type-1 and type-2

FLCs evolved by the GA. The simulation model is described in the Appendix, while the experimental results were obtained using the Kent Ridge Instruments Coupled Tank PP-100. As pointed out in Ref. [37], the volumetric flow rate of the pumps in the coupled-tank apparatus is nonlinear and the system has nonzero transport delay. Besides, the data read by the sensor are noisy. These characteristics are not accurately captured by the model used by the GA to optimize the fuzzy controller parameters. Hence, the ability of the four FLCs to

Table 5
MFs of FLC₁₃, FLC_{2s} and FLC_{2f}.

(a) MFs of e			
	N_e	Z_e	P_e
FLC ₁	-9.0611	6.9846	16.0539
FLC _{2s}	-12.4578	8.6232	12.1405
FLC _{2f}	-12.9137	3.9722	13.1283
	$d_{e_{1r}}=7.0388$	$d_{e_{2l}}=5.0656, d_{e_{2r}}=1.2868$	$d_{e_{3l}}=2.4127$
(b) MFs of \dot{e}			
	$N_{\dot{e}}$	$Z_{\dot{e}}$	$P_{\dot{e}}$
FLC ₁	-0.8093	-0.2884	1.0538
FLC _{2s}	-1.4505	-0.0119	2.1192
FLC _{2f}	-2.0186	$d_{\dot{e}_{2l}}=0.9002, d_{\dot{e}_{2r}}=0.4327$	2.1534
	$d_{\dot{e}_{1r}}=0.5479$	0.6459	
		$d_{\dot{e}_{2l}}=0.7091, d_{\dot{e}_{2r}}=0.5697$	$d_{\dot{e}_{3l}}=0.7644$

Table 6
MFs of FLC₁₅.

(a) MFs of e				
e_1	e_2	e_3	e_4	e_5
-14.8778	-7.5460	-4.7217	7.7783	12.5710
(b) MFs of \dot{e}				
	\dot{e}_2	\dot{e}_3	\dot{e}_4	\dot{e}_5
-1.7824	-0.7799	-0.0387	0.8896	1.7115

handle modeling uncertainties can be ascertained by examining control performances of the FLCs. Using a sampling period of 1 s, step responses were obtained using the four FLCs. Figs. 8 and 9 show the step responses for different setpoints and

the corresponding control signals. The control performances of the four FLCs indicate that they can handle the uncertainties introduced by the pump nonlinearity and the unmodeled transport delay.

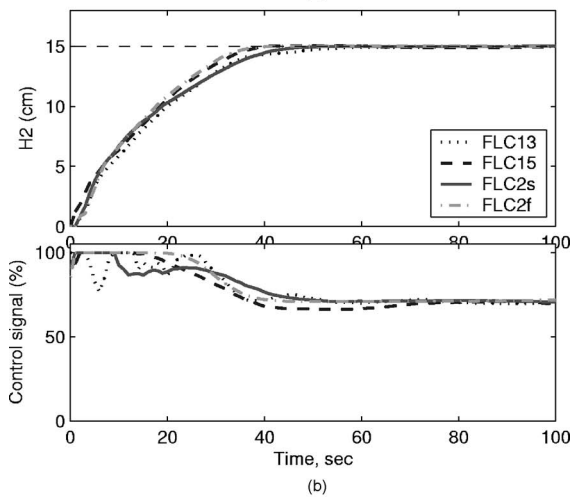
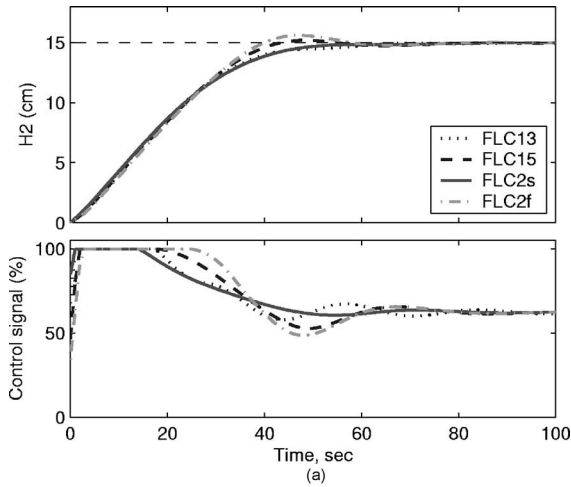


Fig. 8. Step responses when the setpoint was 15 cm. (a) Simulation results and (b) experiment results.

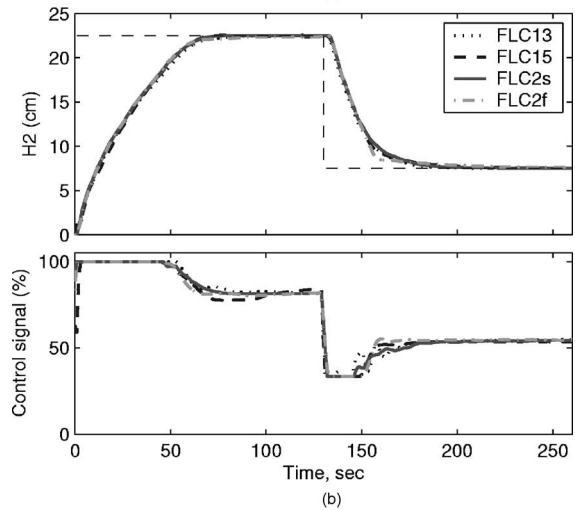
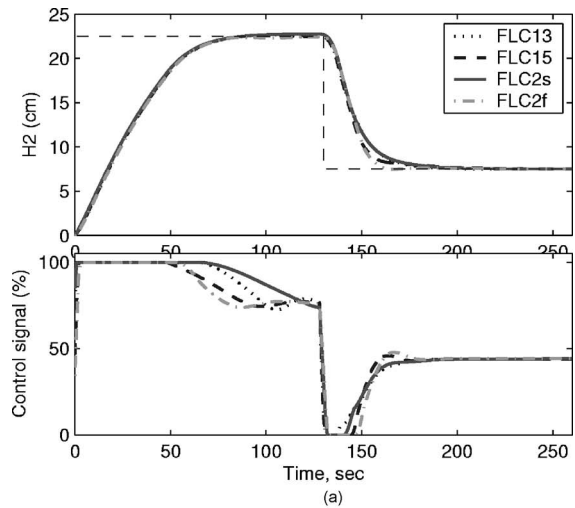


Fig. 9. Step responses when the setpoint was changed. (a) Simulation results and (b) experiment results.

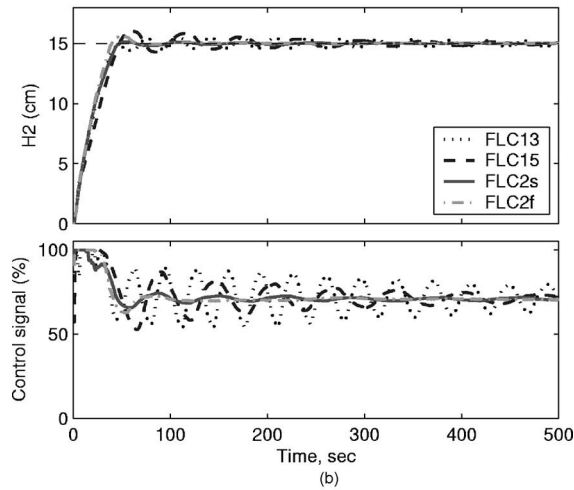
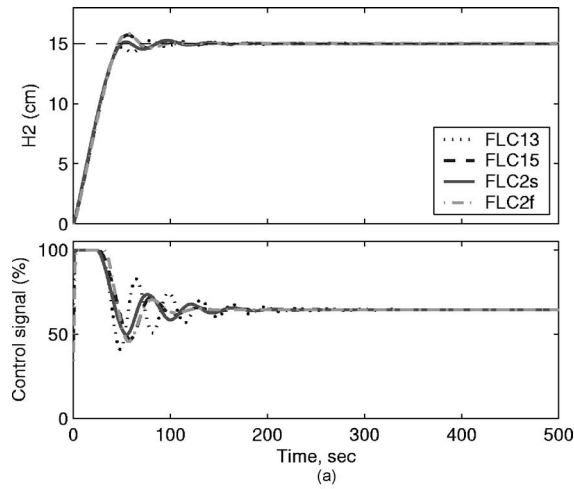


Fig. 10. Step responses when the baffle was lowered. (a) Simulation results and (b) experiment results.

To further test the FLCs, the flow rate between the two tanks was reduced by lowering the baffle separating the two tanks. This change gave rise to a system with slower dynamics. In addition, the difference in liquid level between the two tanks was larger at steady state. When the baffle was lowered, the step responses and the control signals are shown in Fig. 10. It may be observed that although the simulated step responses of the four FLCs are satisfactory, the experimental results corresponding to the two type-1 FLCs (FLC₁₃ and FLC₁₅) exhibit large oscillations. The other two type-2 FLCs have the ability to eliminate these oscillations quickly and the liquid level reaches its desired height at steady state. It is also interesting to notice that the performances of the two type-2 FLCs are similar though they have different number of type-2 MFs.

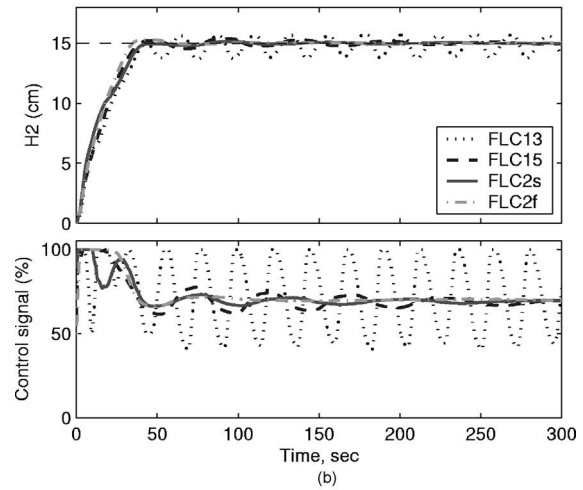
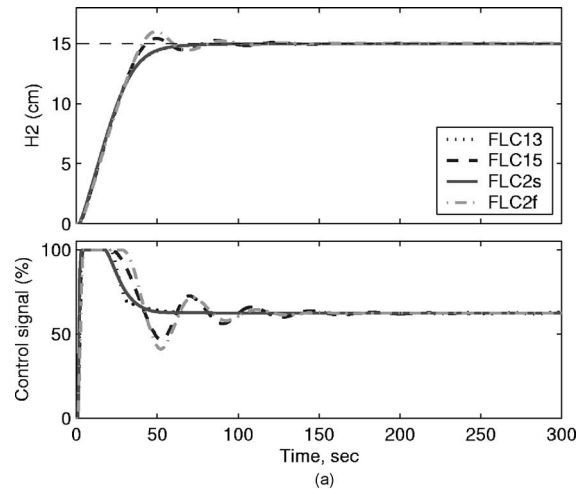


Fig. 11. Step responses when there was a 2 s transport delay. (a) Simulation results and (b) experiment results.

Lastly, the ability of the four FLCs to deal with transport delay was studied and the results are shown in Fig. 11. Once again, both the type-2 FLCs outperform their type-1 counterparts. It is also observed that the performances of the two type-2 FLCs are similar, though they have different number of type-2 MFs. The results suggest that some type-2 MFs may not be necessary and the computational cost may be reduced without sacrificing robustness by using type-1 MFs in place of some type-2 MFs.

5. Discussions

From Figs. 8–11, it may be observed that all four FLCs produced similar simulation results. However, the simulation and experimental results obtained using the type-2 FLCs generally concur

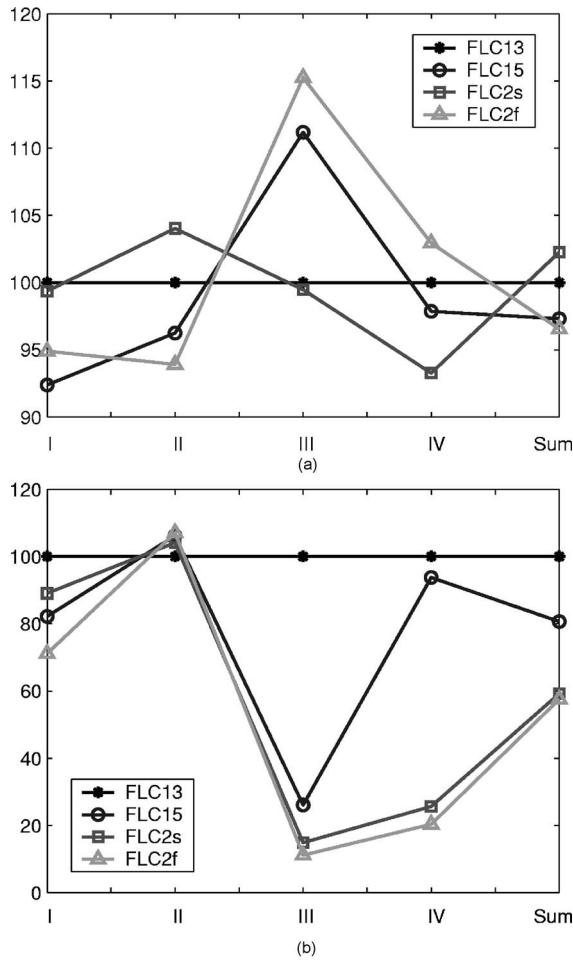


Fig. 12. Comparison of the four FLCs on the four plants. (a) Simulation results; and (b) Experiment results. I, II, III, and IV in horizontal axis stands for plant I, plant II, plant III, and plant IV in Table 4, respectively. Sum means the sum of the ITAEs on the four plants.

more closely than that of the type-1 FLCs. A quantitative measure of the performances of the four FLCs was generated by calculating the ITAE for all cases that were studied. The result is presented in Fig. 12. The plot is scaled such that the ITAEs for the step responses obtain using FLC₁₃ is 100%. Consequently, a smaller number in Fig. 12 translates to a lower ITAE, and therefore better performance. It may be observed that the experimental performances achieved by the two type-2 FLCs are better than that of the type-1 FLCs. Most notably, FLC_{2s} outperforms FLC₁₅ even though FLC₁₅ has six more design parameters.

In common with the standard practice in the GA-based tuning of FLC parameters, a statistical

evaluation was conducted by repeatedly performing the several optimization exercises. Five versions of each controller (FLC₁₃, FLC₁₅, FLC_{2s}, and FLC_{2f}) were evolved and tested on the practical plant. Most of the type-1 FLCs performed poorly. The step responses either had long settling time or exhibited persistent oscillations. FLC₁₃ and FLC₁₅ presented in the previous section actually have the best performance from among the various type-1 FLCs. Several type-2 FLCs from different runs were also tested on the actual plant. The experimental results did not differ from those presented in this paper. This is another indication of the superior ability of type-2 FLCs to tolerate more modeling uncertainties. When a simulation model is used to evaluate the GA candidate solutions, the type-2 FLCs will have a higher probability of performing well on the actual plant.

To further investigate the characteristics of the FLCs, the control surfaces of the four FLCs are generated and shown in Fig. 13. The control surfaces of the two type-2 FLCs are smoother than that of FLC₁₃ around the origin ($e=0$, $\dot{e}=0$). The smoother control surface, especially around the origin, is the reason why the type-2 FLCs are more robust. Note that the control surface of FLC_{2s} is similar to that of FLC_{2f}, even though FLC_{2f} has more type-2 MFs. The control surfaces provide further evidence that there will not be significant performance deterioration when the proposed simplified type-2 FLC is used in place of a traditional type-2 FLC where all the input sets are type-2 MFs.

With the simplified architecture, the computational cost of resulting simplified type-2 FLCs is much lower than that of a traditional type-2 FLC. The time taken by the GA to evolve the four FLCs is shown in Table 7. The data were obtained using a 996 MHz computer with 256 MB of RAM. A 10 000-step simulation [the setpoint is $15 + 10 \sin(i/50)$, where $i=1, 2, \dots, 10\,000$ is the time instant] using the evolved FLCs was also run on the same computer and the computation time is shown in Table 7. The results indicate that the computational cost of FLC_{2s} is much lower when compared with that of FLC_{2f}. The experimental results presented in this paper suggest that the simplified type-2 structure is suitable for real-time implementation. It enables computational cost to

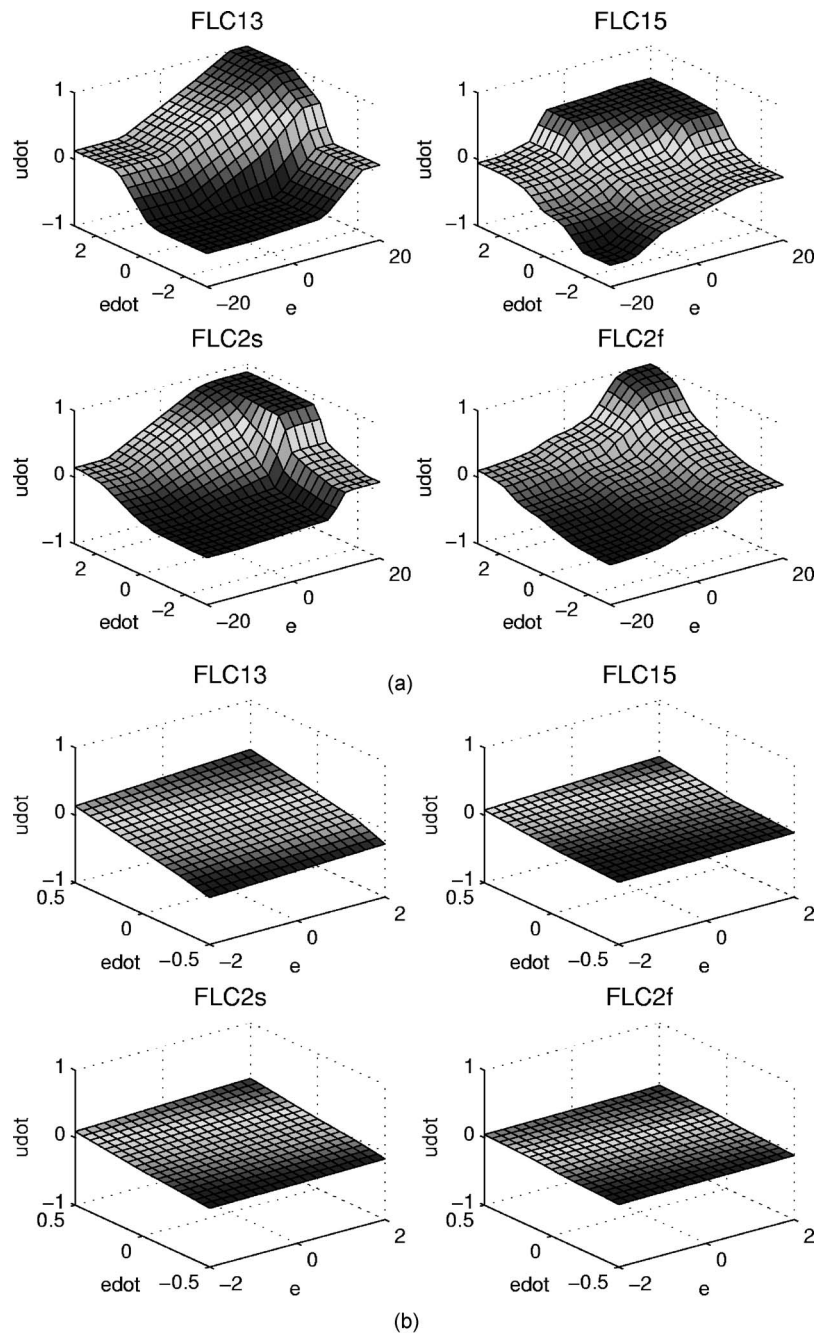


Fig. 13. Control surfaces of the four FLCs. (a) Complete control surfaces and (b) control surfaces near the origin.

be reduced without a degradation in the control performance and the ability to handle modeling uncertainties.

6. Conclusions

In this paper, a simplified type-2 FLC that is more suitable for real-time control is proposed. A

type-2 FLCs with simplified structure are designed for a coupled-tank liquid level control process. Its performance is compared with two type-1 FLCs and a traditional type-2 FLC. Experimental results show that the simplified type-2 FLC outperforms the type-1 FLCs and has similar performance as the traditional type-2 FLC. Analysis also indicates

Table 7
Comparison of computational cost.

Item \ FLC	FLC ₁₃	FLC ₁₅	FLC _{2s}	FLC _{2f}
GA tuning (s)	500	550	1200	4500
Simulation (s)	1.28	1.40	3.19	11.70

there will be at least 50% reduction in computational cost if the simplified type-2 FLC is used in place of a traditional type-2 FLC. It may, therefore, be concluded that the simplified type-2 FLC is able to bring about computational savings without sacrificing the ability to handle modeling uncertainties.

Appendix: The coupled-tank system

The schematic diagram of the coupled-tank system is shown in Fig. 4. The equipment consists of two small tower-type tanks mounted above a reservoir that stores the water. Water is pumped into the top of each tank by two independent pumps, and the levels of water are measured by two capacitive-type probe sensors. Each tank is fitted with an outlet at the side near the base. Raising the baffle between the two tanks allows water to flow between them. The amount of water which returns to the reservoir is approximately proportional to the square root of the height of water in the tank, which is a main source of nonlinearity.

The dynamics of the coupled-tank apparatus can be modeled by the following set of nonlinear differential equations:

$$A_1 \frac{dH_1}{dt} = Q_1 - \alpha_1 \sqrt{H_1} - \alpha_3 \sqrt{H_1 - H_2}, \quad (6a)$$

$$A_2 \frac{dH_2}{dt} = Q_2 - \alpha_2 \sqrt{H_2} + \alpha_3 \sqrt{H_1 - H_2}, \quad (6b)$$

where A_1, A_2 are the cross-sectional area of tank Nos. 1, 2; H_1, H_2 are the liquid level in tank Nos. 1, 2; Q_1, Q_2 are the volumetric flow rate (cm^3/s) of pump Nos. 1, 2; $\alpha_1, \alpha_2, \alpha_3$ are the proportionality constant corresponding to the $\sqrt{H_1}$, $\sqrt{H_2}$, and $\sqrt{H_1 - H_2}$ terms.

The coupled-tank apparatus can be configured as a second-order SISO system by turning off pump No. 2 and using pump No. 1 to control the water level in tank No. 2. Since pump No. 2 is turned off, Q_2 equals zero and Eq. (6b) reduces to

$$A_2 \frac{dH_2}{dt} = -\alpha_2 \sqrt{H_2} + \alpha_3 \sqrt{H_1 - H_2}. \quad (7)$$

Eqs. (6a) and (7) are solved at each sampling instant to generate new liquid levels. The sampling period used to produce the results in this paper is 1 s. It is assumed that the nominal plant has the following process parameters:

$$A_1 = A_2 = 36.52 \text{ cm}^2, \quad (8a)$$

$$\alpha_1 = \alpha_2 = 5.6186, \quad (8b)$$

$$\alpha_3 = 10. \quad (8c)$$

These parameters are the dimensions and discharge coefficients of a Kent Ridge Instruments Coupled Tank PP-100. This test stand is equipped with a direct current voltage supply is $[0, 5]$ V. In this paper the maximum control signal used is 4.906 V, corresponding to an input flow rate of about $75 \text{ cm}^3/\text{s}$. To compensate the dead zone, the minimum control signal is chosen to be 1.646 V, corresponding to the zero input flow rate.

References

- [1] Zadeh, L. A., Fuzzy sets. *Information and Control*. **8**, 338–353 (1965).
- [2] John, J. and Langari, R., *Fuzzy Logic Intelligence, Control and Information*. Prentice Hall, Englewood Cliffs, NJ, 1998.
- [3] Zadeh, L. A., Outline of a new approach to analysis of complex systems and decision processes. *IEEE Trans. Syst. Man Cybern.* **3**, 28–44 (1973).
- [4] King, P. and Mamdani, E., The application of fuzzy control to industrial process. *Automatica* **13**, 235–242 (1977).
- [5] Mendel, J. M., *Rule-Based Fuzzy Logic Systems: Introduction and New Directions*. Prentice-Hall, Englewood Cliffs, NJ, 2001.
- [6] Hagra, H. A., A hierarchical type-2 fuzzy logic control architecture for autonomous mobile robots. *IEEE Trans. Fuzzy Syst.* **12**, 524–539 (2004).
- [7] Zadeh, L. A., The concept of a linguistic variable and its application to approximate reasoning-1. *Information Sciences* **8**, 199–249 (1975).
- [8] Liang, Q. and Mendel, J. M., Interval type-2 fuzzy logic systems: theory and design. *IEEE Trans. Fuzzy Syst.* **8** (5), 535–550 (2000).
- [9] Liang, Q. and Mendel, J. M., Equalization of nonlinear time-varying channels using type-2 fuzzy adaptive filters. *IEEE Trans. Fuzzy Syst.* **8**, 551–563 (2000).
- [10] Liang, Q. and Mendel, J. M., MPEG VBR video traffic modelling and classification using fuzzy technique. *IEEE Trans. Fuzzy Syst.* **9**, 183–193 (2001).
- [11] Yager, R. R., Fuzzy subsets of type-2 in decisions. *Cybernetics* **10**, 137–159 (1980).

- [12] Ozen, T., Garibaldi, J., and Musikasuwan, S., Modeling the variation in human decision making. *Proceedings of the IEEE International Conference on Fuzzy Systems* 2, 617–622 (2004).
- [13] John, R. I., Innocent, P. R., and Barnes, M. R., Neuro-fuzzy clustering of radiographic tibia images using type-2 fuzzy sets. *Information Sciences* 125, 65–82 (2000).
- [14] Mendel, J. M., Fuzzy sets for words: A new beginning. *Proceedings of the IEEE International Conference on Fuzzy Systems* 1, 37–42 (2003).
- [15] Wu, H. and Mendel, J. M., Antecedent connector word models for interval type-2 fuzzy logic systems. *Proceedings of the IEEE International Conference on Fuzzy Systems* 2, 1099–1104 (2004).
- [16] Zeng, J. and Liu, Z.-Q., Type-2 fuzzy hidden markov models to phoneme recognition. *Proceedings of the 17th International Conference on Pattern Recognition* 1, 192–195 (2004).
- [17] Castillo, O. and Melin, P., A new hybrid approach for plant monitoring and diagnostics using type-2 fuzzy logic and fractal theory. *Proceedings of the IEEE International Conference on Fuzzy Systems* 1, 102–107 (2003).
- [18] Melin, P. and Castillo, O., Intelligent control of nonlinear dynamic plants using type-2 fuzzy logic and neural networks. *Proceedings of NAFIPS*, 2002, pp. 22–27.
- [19] Liang, Q., Karnik, N., and Mendel, J. M., Connection admission control in ATM networks using survey-based type-2 fuzzy logic systems. *IEEE Trans. Syst. Man Cybern.* 30 (3), 329–339 (2000).
- [20] Wang, C. H., Cheng, C. S., and Lee, T. T., Dynamical optimal training for interval type-2 fuzzy neural network (T2FNN). *IEEE Trans. Syst. Man Cybern.* 34, 1462–1477 (2004).
- [21] Lee, C.-H. and Lin, Y.-C., Control of nonlinear uncertain systems using type-2 fuzzy neural network and adaptive filter. *Proceedings of the IEEE International Conference on Networking, Sensing and Control* 2, 1177–1182 (2004).
- [22] Tan, W. W. and Pall, S. N., Performance study of type-2 fuzzy controllers. *Proceedings of the 2nd International Conference on Computational Intelligence, Robotics and Autonomous Systems*, 2003.
- [23] Wu, D. R. and Tan, W. W., A type-2 fuzzy logic controller for the liquid-level process. *Proceedings of the IEEE International Conference on Fuzzy systems* 2, 953–958 (2004).
- [24] Wu, D. R. and Tan, W. W., A simplified architecture for type-2 FLSs and its application to nonlinear control. *Proceedings of the IEEE Conference on Cybernetics and Intelligent Systems*, 2004, pp. 485–490.
- [25] Wu, H. and Mendel, J. M., Uncertainty bounds and their use in the design of interval type-2 fuzzy logic systems. *IEEE Trans. Fuzzy Syst.* 10, 622–639 (2002).
- [26] Wu, D. R. and Tan, W. W., Computationally efficient type-reduction strategies for a type-2 fuzzy logic controller. *Proceedings of the IEEE International Conference on Fuzzy Systems*, 2005, pp. 353–358.
- [27] Karnik, N. N., Liang, Q., and Mendel, J. M., Type-2 fuzzy logic software, 2000, <http://sipi.usc.edu/mendel/software/>.
- [28] Holland, J., *Adaptation in Natural and Artificial Systems*. University of Michigan Press, Ann Arbor, MI, 1975.
- [29] Goldberg, D. E., *Genetic Algorithms in Search, Optimization and Machine Learning*. Addison-Wesley, New York, 1989.
- [30] Michalewicz, Z., *Genetic Algorithms + Data Structures = Evolution Programs*. Springer-Verlag, New York, 1996.
- [31] Man, K., Tang, K., Kwong, S., and Halang, W., *Genetic Algorithms for Control and Signal Processing*. Springer, New York, 1997.
- [32] Sakawa, M., *Genetic Algorithms and Fuzzy Multiobjective Optimization*. Kluwer Academic, Boston, 2002.
- [33] Kim, J., Moon, Y., and Zeigler, B., Designing fuzzy net controllers using genetic algorithms. *IEEE Control Syst. Mag.* 15, 66–72 (1995).
- [34] Homaifar, A. and McCormick, E., Simultaneous design of membership functions and rule sets for fuzzy controllers using genetic algorithms. *IEEE Trans. Fuzzy Syst.* 3, 129–138 (1995).
- [35] Cordon, O., Herrera, F., Hoffmann, F., and Magdalena, L., *Genetic Fuzzy System: Evolutionary Tuning and Learning of Fuzzy Knowledge Bases*. World Scientific, Singapore, 2001.
- [36] Cordon, O., Herrera, F., Gomide, F., Hoffmann, F., and Magdalena, L., Genetic fuzzy systems: New developments. *Fuzzy Sets Syst.* 141, 1–163 (2004).
- [37] Teo, L., Khalid, M., and Yusof, R., Self-tuning neuro-fuzzy control by genetic algorithms with an application to a coupled-tank liquid-level control system. *Eng. Applic. Artif. Intell.* 11, 517–529 (1998).

Dongrui Wu received a B.E in automatic control from the University of Science and Technology of China in 2003, and a M.Eng in electrical engineering from the National University of Singapore in 2005. Currently he is pursuing his Ph.D. in electrical engineering at the University of Southern California. He received the Best Student Paper Award in IEEE International Conference on Fuzzy Systems, Reno, Nevada, 2005. His research interests are computational intelligence and its application to smart oilfield technology.

Woei Wan Tan graduated with a Bachelor of Engineering (electrical, honors) degree and a Master of Engineering degree from the National University of Singapore in 1993 and 1995, respectively. After receiving a Doctor of Philosophy degree from Oxford University for her work in self-learning neurofuzzy control of nonlinear systems in December 1997, she returned to the National University of Singapore as an assistant professor. Her research program focuses on the application of systems science and computational intelligence paradigms for controller design, metrology, and fault detection and diagnosis. In particular, she has published papers on: (i) intelligent modeling, control and fault diagnosis using computational intelligence techniques, (ii) application of advanced control algorithms to the semiconductor manufacturing industry, (iii) microelectromechanical pressure sensors, and (iv) autotuning of multivariable systems.